J Physiol 587.2 (2009) pp 491–504

The Journal of Physiology

Threshold behaviour of human axons explored using subthreshold perturbations to membrane potential

David Burke[1], James Howells[1], Louise Trevillion[1], Penelope A. McNulty[1], Stacey K. Jankelowitz[1] and Matthew C. Kiernan[2]

[1] *Institute of Clinical Neurosciences, Royal Prince Alfred Hospital and The University of Sydney, Sydney, Australia*
[2] *Prince of Wales Medical Research Institute and Prince of Wales Clinical School, University of New South Wales, Sydney, Australia*

The present study explores the threshold behaviour of human axons and the mechanisms contributing to this behaviour. The changes in excitability of cutaneous afferents in the median nerve at the wrist were recorded to a long-lasting subthreshold conditioning stimulus, with a waveform designed to maximize the contribution of currents active in the just-subthreshold region. The conditioning stimulus produced a decrease in threshold that developed over 3–5 ms following the end of the depolarization and then decayed slowly, in a pattern similar to the recovery of axonal excitability following a discharge. To ensure that the conditioning stimulus did not activate low-threshold axons, similar recordings were then made from single motor axons in the ulnar nerve at the elbow. The findings were comparable, and behaviour with the same pattern and time course could be reproduced by subthreshold stimuli in a model of the human axon. In motor axons, subthreshold depolarizing stimuli, 1 ms long, produced a similar increase in excitability, but the late hyperpolarizing deflection was less prominent. This behaviour was again reproduced by the model axon and could be explained by the passive properties of the nodal membrane and conventional Na^+ and K^+ currents. The modelling studies emphasized the importance of leak current through the Barrett–Barrett resistance, even in the subthreshold region, and suggested a significant contribution of K^+ currents to the threshold behaviour of axons. While the gating of slow K^+ channels is slow, the resultant current may not be slow if there are substantial changes in membrane potential. By extrapolation, we suggest that, when human axons discharge, nodal slow K^+ currents will be activated sufficiently early to contribute to the early changes in excitability following the action potential.

(Received 9 September 2008; accepted after revision 26 November 2008; first published online 1 December 2008)
Corresponding author D. Burke. Medical Foundation Building - K25, The University of Sydney, Sydney, N.S.W. 2006, Australia. Email: d.burke@med.usyd.edu.au

With the advent of reliable threshold-tracking techniques (Bostock *et al.* 1998; Kiernan *et al.* 2000) considerable insight has been obtained into the mechanisms governing the excitability of human axons in health (Burke *et al.* 2001) and disease (Lin *et al.* 2006; Krishnan *et al.* 2008). The excitability of an axon determines the basis on which action potentials are generated, and depends on the resting membrane potential. This is, in turn, determined by (i) voltage-dependent conductances active at rest (including persistent Na^+ current (I_{NaP}), slow K^+ currents (I_{Ks}), some fast K^+ currents (I_{Kf}), and non-specified leak conductances), (ii) currents that are not voltage dependent (including flicker; ATP- and Ca^{2+}-responsive) and (iii) current generated by the electrogenic Na^+/K^+ pump (see Ritchie, 1995; Bostock *et al.* 1998; Burke *et al.* 2001).

An important role for a persistent (late) Na^+ current (I_{NaP}) in the threshold behaviour of human myelinated axons has been inferred from the studies of Bostock & Rothwell (1997) and Hales *et al.* (2004). However, when subthreshold changes in excitability of axons were explored using brief depolarizing current pulses, the contribution of I_{NaP} to subthreshold superexcitability was much less than that attributable to the cable properties of the myelinated axon (Bostock *et al.* 2005; see also Shefner *et al.* 1996). This might have been anticipated: the phase of supernormality (or superexcitability) produced by a conditioning stimulus that is suprathreshold is largely due to cable properties of the axon, specifically passive depolarization of the internodal axolemma by current leaking through or under the myelin sheath (the 'Barrett–Barrett' current; see Barrett & Barrett, 1982; Blight, 1985; Blight & Someya, 1985; Bowe *et al.* 1987; Ritchie, 1995). However, even following a discharge, the passive depolarization is likely to be augmented by I_{NaP}

DOI: 10.1113/jphysiol.2008.163170

(McIntyre *et al.* 2002), a conclusion supported by human experiments (Bostock *et al.* 2005).

The question then arises whether other currents contribute significantly to the excitability of axons in the just-subthreshold region. This might be expected given that ~35% slow K^+ channels are open at resting membrane potential (Röper & Schwarz, 1989; see Baker *et al.* 1987), and that slow K^+ currents are responsible for accommodation to subthreshold depolarizing currents in threshold electrotonus (Bostock *et al.* 1998). To explore this question further for human myelinated axons *in vivo*, membrane potential was disturbed by a long-lasting subthreshold conditioning stimulus, designed to maximize currents potentially active in the just-subthreshold region. Using threshold tracking, we measured the changes in excitability at different conditioning–test intervals, and demonstrate a pattern of 'subthreshold superexcitability' that resembles the recovery of excitability following a discharge (the 'recovery cycle'). As the conditioning–test interval increased, the decrease in threshold was increasingly offset by an outwardly rectifying threshold change due to K^+ currents, much as in a recovery cycle. Mathematical modelling indicated that passive electrotonic behaviour dominates stimulus-induced changes in excitability, not only when an axon discharges, but also in the subthreshold region. In addition we argue that, *in vivo*, the current through a channel may follow more closely the change in membrane potential than the time course of channel gating.

Methods

The behaviour of cutaneous afferent axons was studied by recording compound sensory action potentials (CSAPs) in 24 experiments on five healthy volunteers (2 male, 3 female; aged 35–61 years) who had no evidence of a neurological disturbance. The behaviour of single motor units was studied in 23 experiments on three of the five volunteers. It should be noted that, while there may be significant age- and gender-related differences in impulse conduction along a nerve, there are only minor differences, if any, in axonal excitability measured using threshold tracking (e.g. Kiernan *et al.* 2001; Jankelowitz *et al.* 2007*b*; Bae *et al.* 2008). Informed written consent was obtained, and experiments were conducted in accordance with the *Declaration of Helsinki* and with the approval of The University of Sydney Human Research Ethics Committee.

In these experiments, the threshold for a group of axons (with CSAPs) or a single axon (with single motor units) was taken as an indirect measure of membrane potential. With CSAPs, threshold was the current that produced a compound potential that was 50% of maximum. With the single motor units, threshold was the stimulus current that discharged the axon on 50% of presentations. In all experiments, the relevant threshold was measured each stimulus cycle and changes in threshold were determined as percentage deviations from this value, cycle by cycle.

In the present studies stimuli were delivered to the median nerve at the wrist or the ulnar nerve at the elbow, where the nerves are superficial.

Compound sensory action potentials

The median nerve was stimulated at the wrist via Ag–AgCl adhesive surface electrodes, the cathode 1 cm proximal to the wrist crease and anode a further ~10 cm proximal over muscle. Antidromic compound sensory action potentials (CSAPs) were recorded from the index finger using ring electrodes. The potentials were amplified and filtered (3 Hz–3 kHz; ICP511 AC amplifier, Grass Product Group, West Warwick, RI, USA) and digitized by a computer with a 16-bit analog-to-digital board (PCI-6621M, National Instruments, Austin, TX, USA) using a 10 kHz sampling rate.

Conditioning and test stimuli were delivered by a purpose-built isolated constant-current stimulator controlled by a computer running QTRAC (Professor H. Bostock, Institute of Neurology, London), delivering a regularly repeating sequence of conditioning and test stimuli. The study involved measuring the effects of conditioning stimuli on the excitability of sensory axons, as measured by the change in threshold for a submaximal test CSAP, normalized to the unconditioned (control) threshold. The experiments used a complex three-pulse conditioning stimulus (Fig. 1*A*). The three-pulse stimulus was chosen to enhance Na^+ currents and, by holding the axons in a partially depolarized state, to augment other voltage-dependent conductances. The conditioning stimulus began with hyperpolarization designed to diminish resting inactivation of Na^+ channels, and was set so that it would produce little activation, if any, of the hyperpolarization-activated conductance, I_H. The subsequent depolarizing pulse was set so that it just failed to activate axons directly, i.e. to be just subthreshold. The third pulse consisted of a sustained but weaker level of depolarization. By holding axons partially depolarized relative to the resting state, it was intended that voltage-dependent channels would not immediately close and the effects of those with slow gating could become apparent. Subcutaneous tissue may have filtered the current waveform reaching axons but this would not be a confounding factor in the present studies. However, it might help explain the scaling differences between the recorded data and the behaviour of our mathematical model of the human myelinated axon.

In different experiments, the duration of the depolarizing pulse of the conditioning stimulus was varied. It was critical that this stimulus always remained

subthreshold, and the initial experiments on CSAPs focused on a 1 ms wide depolarizing pulse. In experiments using 5 ms and 10 ms wide pulses, the strength of the pulse was matched to that of the 1 ms pulse (see later). As shown in Fig. 1*A*, and explained earlier, the three pulses of the conditioning stimulus were: (i) a 5 ms hyperpolarizing pre-pulse that was set to −30% of the 1 ms threshold for a CSAP that was 50% of maximal amplitude; (ii) a 'brief' depolarizing pulse of 1 ms, 5 ms or 10 ms duration set to be just subthreshold (see below); and (iii) a long-lasting partially depolarizing pulse set to half the intensity of the 1 ms depolarizing pulse (even when its duration was increased to 5 or 10 ms). This pulse was held for longer than the longest conditioning–test interval (19–20 ms from the end of the depolarizing pulse for the CSAP recordings). To ensure that components (ii) and (iii) of the conditioning stimulus did not activate low-threshold sensory axons, 10 sweeps of the neural recording were averaged online.

The effect of this complex conditioning stimulus on axonal excitability was measured by tracking the threshold for the test potential. The test stimulus was 0.1 ms in duration. The threshold for the test potential was determined at 15 intervals from 1 to 19 ms after the end of the brief depolarizing pulse (i.e. after (ii) in Fig. 1*A*). To isolate the change in threshold due to the depolarizing pulse, it was necessary to remove the effects due to threshold electrotonus produced by the long-lasting partially depolarizing pulse of the conditioning stimulus (open symbols in Fig. 1*C*). The response to the depolarizing pulse was normalized to the changes in threshold when the depolarizing pulse in the conditioning stimulus was reduced to the same level as the partially depolarizing pulse, so that the long-lasting partial depolarization began 1, 5 or 10 ms earlier, at the end of the hyperpolarizing pre-pulse (i.e. as in Fig. 1*B*).

When the protocol was run with depolarizing pulses lasting 5 ms and 10 ms, the amplitude of the longer depolarizing pulse was calculated from the 1 ms pulse using the strength–duration properties of the test CSAP. This prevented direct activation of axons by the conditioning stimulus. The strength–duration time constant was measured using the Trond protocol of QTRAC immediately before running the 5 ms and 10 ms protocols. The initial hyperpolarization and the long-lasting partial depolarization were not changed, i.e. −30% of threshold and +50% of the stimulus intensity of a 1 ms just-subthreshold depolarizing pulse, respectively.

Single motor axons

The responses of single motor units were recorded because the presence or absence of an all-or-none single motor unit potential of constant latency provides unequivocal evidence of whether the stimulus is truly subthreshold. The responses of sensory and motor axons to external stimuli are qualitatively similar, though there are quantitative differences, due in part to differences in channel expression, including I_{NaP} (Mogyoros *et al.* 1996; Bostock & Rothwell, 1997; Bostock *et al.* 1998; Burke *et al.* 2001). Accordingly, with single motor axons we expected equivalent conditioning stimuli to produce basically similar responses but of different magnitude.

The ulnar nerve was stimulated using Ag–AgCl adhesive surface electrodes, with the cathode at the cubital tunnel, and the anode ∼10 cm more proximal over the triceps muscle. Surface EMG was recorded from flexor carpi ulnaris, using a single differential, parallel-bar EMG sensor (DE2.3 Myomonitor, Delsys, Boston, MA, USA). With such electrodes, low-threshold single motor units can be isolated, whether during voluntary activity (Iglesias *et al.* 2007) or with graded electrical stimuli (Bostock *et al.* 2005; see Fig. 4). Again, electrical stimuli were delivered from the constant-current stimulator controlled by a computer running QTRAC. The motor unit discharges were amplified using a purpose-built amplifier and digitized using the same data acquisition card as before. The threshold for the single unit was defined as the stimulus intensity that elicited a discharge on 50% of presentations and, as with CSAP recordings, the protocol measured the changes in threshold produced by the conditioning stimulus.

The conditioning stimulus consisted of three sequential pulses: (i) a 10 ms hyperpolarizing pre-pulse set to −30% of the 1 ms threshold for the motor unit discharge; (ii) a 5 ms depolarizing pulse set to an intensity that was 94% of the threshold for the motor unit discharge; and (iii) a sustained depolarization at half the intensity of the depolarizing pulse, maintained for up to 40 ms. The response to the test stimulus was measured at 26 intervals between 0.1 ms and 40 ms from the offset of the depolarizing pulse, with particular focus on the first 5 ms. The changes produced by the depolarizing pulse were defined by subtracting the changes produced by a conditioning stimulus in which the depolarizing pulse was equal in magnitude to the long-lasting partially depolarizing pulse (as for CSAPs).

To identify any contribution of the different pulses of the complex subthreshold conditioning stimulus to the threshold changes, the conditioning stimulus was modified by removing the hyperpolarizing pre-pulse and the long-lasting partial depolarization, so that it consisted of only the subthreshold depolarizing pulse. The protocol was run using conditioning stimuli of 0.1, 1, 5 and 10 ms duration, each set to 94% of the threshold for the motor unit to that stimulus duration. Again, the threshold for the test potential was measured at 25 intervals up to 40 ms from the falling edge of the depolarizing pulse.

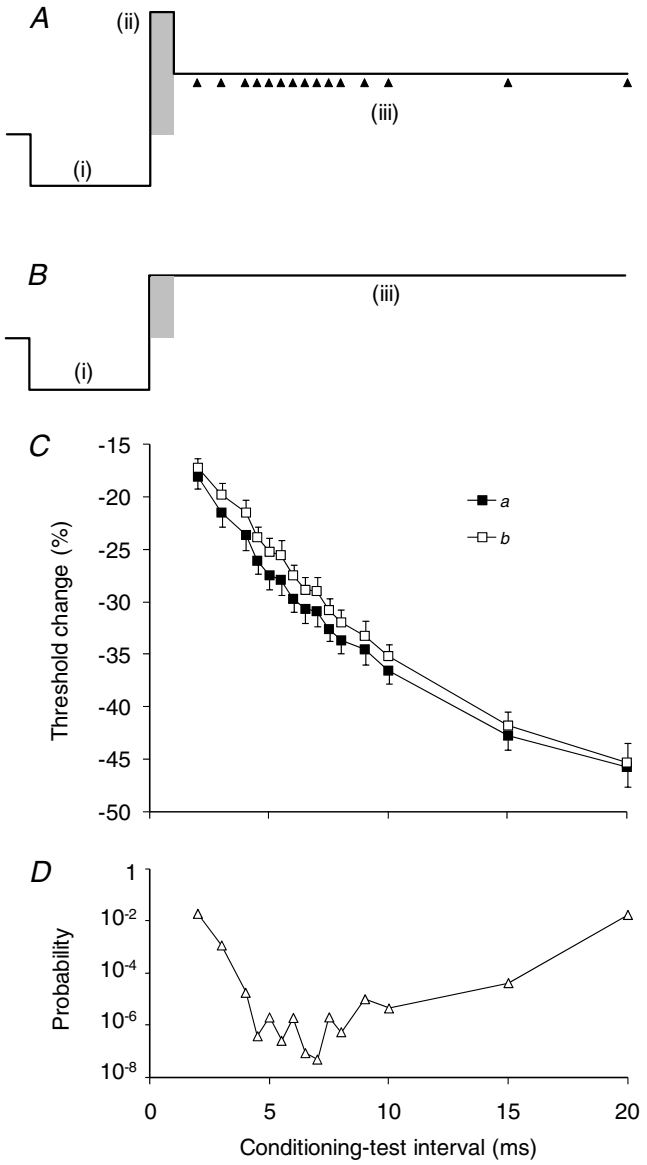

Figure 1. Threshold changes in sensory axons in response to a conditioning stimulus
A, the conditioning stimulus consisted of 3 phases: (i) a 5-ms-long hyperpolarizing 'pre-pulse', the strength of which was −30% of the threshold for the test CSAP as measured using a 1 ms depolarizing stimulus; (ii) a depolarizing pulse that lasted 1, 5 or 10 ms (1 ms in this figure: shaded), the strength of which was just below that for a detectable CSAP; and (iii) a long-lasting depolarizing pulse that was half the strength of the preceding depolarizing pulse so that axons were maintained partially depolarized. Threshold was tested at different conditioning–test intervals starting 1 ms after the end of the depolarizing pulse, as indicated by the arrowheads. *B*, the conditioning stimulus without the depolarizing pulse (ii). *C*, changes in threshold for a 0.1 ms test stimulus recorded from sensory axons in response to the conditioning stimuli in *A* (■) and *B* (□). Data for one subject (mean ± S.E.M.; 10 experiments). The normalized difference between these plots represents the response to the 1 ms depolarizing pulse, and this is illustrated in subsequent figures. *D*, changes in the *P* value when the threshold changes induced by conditioning stimulus *A* are compared with those induced by conditioning stimulus *B* (Student's paired *t* test, without Bonferroni correction).

Mathematical model of the human motor axon

The mathematical model (the 'Bostock model') is based on a single node and internode connected by an internodal leak pathway (the Barrett–Barrett resistance), as used to explain electrotonus in rat and human motor axons (Bostock & Baker, 1988). It was subsequently developed by Bostock *et al.* (1991), described in detail in Hales *et al.* (2004) and applied in studies on patients (e.g. Bostock *et al.* 1995; Kiernan *et al.* 2005; Kanai *et al.* 2006; Jankelowitz *et al.* 2007*a*). The voltage-clamp data of Schwarz *et al.* (1995) were used to model transient Na^+ channels. Persistent Na^+ currents were modelled as non-inactivating channels with a threshold 18 mV lower. Both the node and internode contain different ohmic leak conductances and electrogenic pump currents. The model does not include an open-blocked state for Na^+ channels, introduced by Raman & Bean (2001), to account for resurgent Na^+ current, but this is unlikely to be relevant for the present study because subthreshold depolarizing stimuli would not generate a resurgent Na^+ current on partial repolarization.

The changes in threshold of the model motor axon in response to the conditioning stimuli used on single motor units in the present study was determined as the test stimulus that evoked an all-or-none discharge (Figs 5 and 6). The changes in membrane potential and in the relevant ionic currents underlying the recorded behaviour were explored (Fig. 7). The effects of reducing I_{Ks} on the action potential and the recovery cycle of the model motor axon were measured when resting membrane potential was not controlled ('unclamped') and when the pre-stimulus level was restored to resting level (−83.15 mV) by adjustment of the pump current (Fig. 8).

Data analysis

Data are presented as mean ± S.E.M. The reproducibility of the small changes in the CSAP are shown for a single subject in Figs 1 and 2 (open circles) and 3, and between subjects in Fig. 2 (filled circles). The grand average for the five subjects in Fig. 2 (filled circles) was calculated as the mean ± S.E.M. of the average findings for each subject. Significance was determined using Student's *t* test, and values are given in the text with Bonferroni correction, when appropriate. A corrected probability of < 0.05 was considered significant.

Results

Responses of cutaneous afferent axons

In Fig. 1 the changes in threshold produced by the complex conditioning stimulus in panel *A* are shown in *C* (*a*, filled squares). The response to the depolarizing pulse was identified by subtracting the changes in threshold

produced by the stimulus in panel *B* from those to the stimulus in *A*, and can be appreciated as the difference between the plots in *C*. The differences were small, some 2–3%, particularly when compared with the trial-to-trial variability (see error bars in *C*). However, the difference was present in each recording, and became significant at 2 ms ($P < 0.02$; paired Student's *t* test with Bonferroni correction; $N = 15$). The difference was maximal at 5–6 ms where the corrected probability was $< 0.2 \times 10^{-4}$. Figure 1*D* plots the significance of these differences (without the Bonferroni correction). It should be noted that, while the threshold change attributable to the 1 ms wide depolarizing pulse is small, it is numerically greater than the variability of the threshold of single motor units (Hales *et al.* 2004) and the proportion of the total Na^+ current believed to be persistent (Bostock & Rothwell, 1997), emphasizing that, in the threshold region, small currents can produce profound changes.

The 1 ms depolarizing pulse in the complex conditioning stimulus produced a decrease in threshold for the test CSAP, up to ∼3% of the control threshold, 4–6 ms after the end of the depolarizing pulse, with decay to control levels over 15–20 ms (Fig. 2*A*). The pattern was superficially similar to the recovery of excitability following a conditioning discharge (Fig. 2*B*). The major differences between Fig. 2*A* and *B* are (i) the magnitude of the threshold changes, and (ii) the overt refractoriness in the recovery cycle in *B*.

The gradual development of the full threshold decrease with subthreshold conditioning stimuli in Fig. 2*A* is not that expected from a tail current (which should be maximal immediately or shortly after the repolarizing edge of the pulse; see Raman & Bean, 2001; Magistretti *et al.* 2006). The time course is similar to that described for a resurgent Na^+ current in neurones (Raman & Bean, 1997, 2001). However, subthreshold stimuli would not have caused the axons to enter the voltage regions optimal for resurgent currents, which typically require strong depolarization to +30 or +40 mV with repolarization to −40 mV (see Raman & Bean, 1997, 2001). A more plausible explanation is that the stimulus was above threshold for some low-threshold axons contributing to the CSAP, and that averaging the sensory recording against the conditioning stimulus had failed to reveal this. The gradual development of the decrease in threshold would then result from decaying refractoriness in these axons as they passed through a recovery cycle (as illustrated in Fig. 2*B*).

In addition to averaging the CSAP, three approaches were adopted to address the question of whether the conditioning stimulus was truly subthreshold. First, it was reasoned that the gradual onset should become less apparent with depolarizing pulses of longer duration because pulses of similar strength but longer duration would be of lower amplitude, and any inadvertent direct activation by the conditioning stimulus would be either locked to the onset of the depolarization or dispersed throughout the longer-duration depolarizing pulse. Second, recordings were made from single motor units in response to comparable conditioning stimuli. Third, the data were reproduced in a mathematical model of the human motor axon (Bostock *et al.* 1991; Bostock & Rothwell, 1997; Hales *et al.* 2004).

Depolarizing pulses of different duration

The duration of the depolarizing pulse in the conditioning waveform was increased but kept just-subthreshold by

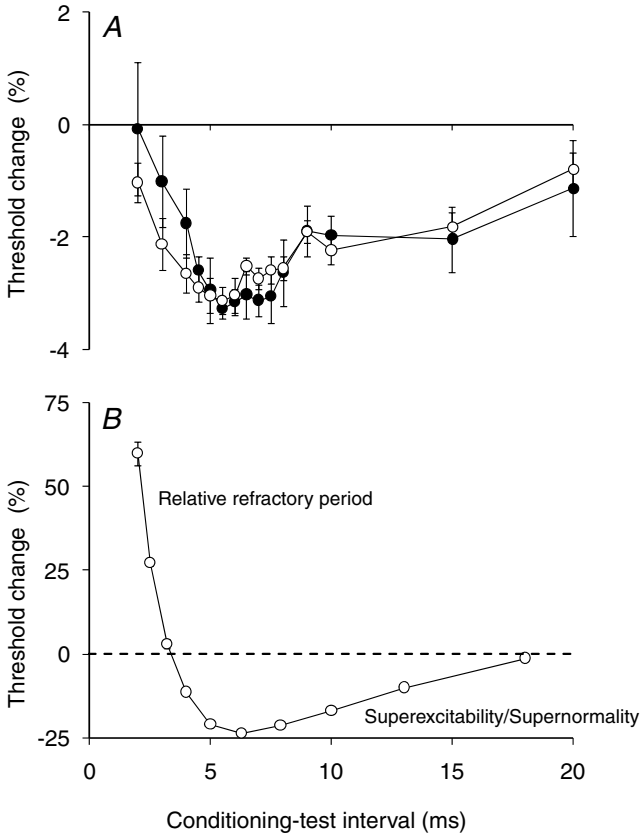

Figure 2. Threshold changes in sensory axons in response to the depolarizing pulse of the conditioning stimulus
A, changes in excitability recorded from sensory axons in response to the conditioning stimulus (produced by a 0.1 ms test stimulus). To extract the response to the depolarizing pulse ((ii) in Fig. 1*A*), separate from the threshold electrotonic response to the repolarization pulse ((iii) in Fig. 1*A*), the threshold changes to the waveform in Fig. 1*B* were subtracted from those to Fig. 1*A*, and are displayed. Data for a single subject (○; mean ± S.E.M.; 10 experiments) and for five subjects (●; mean ± S.E.M.; incorporating the mean data for the single subject) are shown. Here and in Figs 1 and 3, zero on the *x*-axis reflects the onset of the 1 ms depolarizing pulse. *B*, recovery of excitability of sensory axons following a maximal conditioning discharge. Mean of 5 recordings ± S.E.M. Data for the subject (○) in *A*. Note that the symbols are larger than the error bars at all intervals except 2 ms.

an equivalent amount for each pulse width. To keep the strength of the depolarizing pulses equivalent, the strength–duration properties for sensory axons were measured. Based on Weiss' formula (Weiss, 1901; Bostock, 1983; Mogyoros *et al.* 1996), the 5 ms and 10 ms current pulses were set so that they were just-subthreshold, by the equivalent extent as with the 1 ms pulse. As such, these wider pulses were of smaller amplitude but greater charge. The strength of the other two components of the conditioning stimulus, the 'pre-pulse' and the long-lasting partial depolarization, were not changed; they remained identical to those with the 1 ms depolarizing pulse.

The decrease in threshold was related to the end of the depolarizing pulse, not its onset (Fig. 3). It became greater in depth and shifted in time as the duration of the depolarizing pulse in the conditioning stimulus was increased (Fig. 3). The onset of the decrease in threshold was similar when the depolarizing pulses were of different duration, with a maximal threshold decrease ∼4–5 ms after the end of the pulse. However, the subsequent decay became more rapid as a late hyperpolarizing threshold change became superimposed on the threshold decrease (Fig. 3), suggesting that the longer pulse more effectively activated a hyperpolarizing conductance. This change can be explained by more effective activation of K^+ conductances, as would be expected with depolarizing currents of longer duration. The gradual onset of the threshold decrease cannot be attributed to the slow depolarizing ('S1') phase of threshold electrotonus, which is illustrated in trace *b* in Fig. 1*C*. The response to the depolarizing pulse was measured as the difference between traces *a* and *b* in Fig. 1*C*.

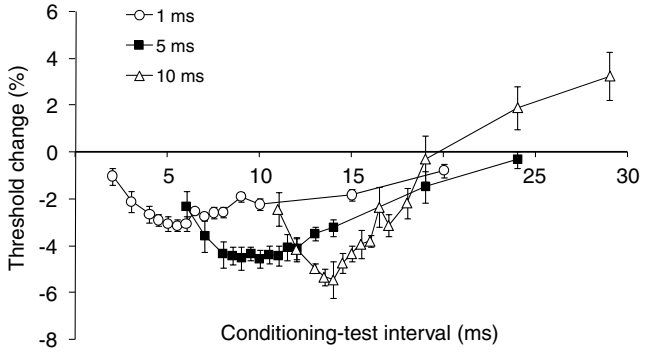

Figure 3. Threshold changes in sensory axons as the duration of the depolarizing pulse in the conditioning stimulus was increased

Threshold changes recorded from sensory axons of a single subject in response to the same complex conditioning stimulus presented in Fig. 2, except that the depolarizing pulse was increased in duration from 1 ms (○; data also presented in Fig. 2; mean ± S.E.M.; 10 experiments) to 5 ms (■; mean ± S.E.M.; 5 experiments) and 10 ms (△; mean ± S.E.M.; 5 experiments). As in Figs 1 and 2, the depolarizing pulses began at zero on *x*-axis, and measurements were started 1 ms after it ended. Strength–duration properties were used to calculate the stimulus current for the 5 ms and 10 ms pulses to ensure they were subthreshold and of equivalent strength to the 1 ms pulse. Changes in the threshold of the test potential were measured using a 0.1 ms wide test stimulus.

At first sight the latency shift could imply that the gradually developing threshold decrease was a response to the offset of the depolarizing pulse of the conditioning stimulus (much as is the case with resurgent current). However, the threshold change would be related to the end of the depolarizing pulse if it was dependent on the total charge in the pulse. Changes in excitability due to the cable properties of the axon should increase with stimulus charge, but those due to Na^+ currents should be related to stimulus current (Bostock *et al.* 2005). The growth of the subthreshold superexcitability and its shift in latency with longer stimulus durations are evidence for an important contribution of the passive electrotonic properties of the myelinated axon to the threshold decrease.

Responses of single motor units

Figure 4 illustrates the ability to distinguish reliably the activity of single motor units using the differential parallel-bar sensor, showing, in panels *D–F*, the entire experimental data for one of the experiments in Fig. 5*A*. Panels *A* and *B* of Fig. 4 show the all-or-none behaviour of the single motor unit, unconditioned (*A*) and conditioned (*B*). Figure 4*C* shows the identity of the waveforms when the artefact in *B* due to the conditioning stimulus was subtracted out. Note that in *C* the conditioned test stimulus was offset by 1 ms so that the waveforms in *C* could be distinguished. Panels *D* and *E* illustrate the amplitude of the all-or-none responses for that unit (the 'hits' in the upper row and the 'misses' in the lower row) for the entire experiment to indicate the fidelity of triggering (*D* unconditioned; *E* conditioned) with the trigger level indicated by the dashed line. The data points for the traces in *A* and *B* are indicated by the filled circles. Panel *F* shows the latency of the motor unit potential in the upper rows of *D* (unfilled circles) and *E* (filled circles).

For single motor units, the width of the depolarizing pulse of the 3-pulse conditioning stimulus was 5 ms, because 5 ms produced greater threshold changes for sensory axons than 1 ms. Its strength was adjusted to 94% of the threshold for the motor axon measured using a 5-ms-long test stimulus. Given that the coefficient of variation of threshold variability for human motor axons is ∼1.65% (Hales *et al.* 2004), the 94% intensity ensured that the depolarizing pulse remained just-subthreshold. To define more clearly the onset of the decrease in threshold in these studies, measurements were made more frequently, starting on the falling (repolarizing) edge of the depolarizing pulse.

The complex conditioning stimulus was used in three subjects, and consistent responses were seen in all

recordings. Figure 5*A* illustrates the average data from the three units. The threshold changes were qualitatively similar to those of sensory axons: (i) the gradual onset of the increase in excitability and (ii) the subsequent decay into hypoexcitability. The differences relate primarily to the timing of the different phases. This may be due to a number of factors: (i) the motor unit data involved the behaviour of a single low-threshold axon rather than a compound response, (ii) the conditioning stimuli were not identical, and (iii) there are differences in channel expression for human sensory and motor axons (Bostock & Rothwell, 1997; Bostock *et al.* 1998; Burke *et al.* 2001). There was a gradually developing increase in excitability, with maximal decrease in threshold of ∼17% at 3–4 ms (as against 4–6 ms for sensory axons), followed by a decrease in excitability (Fig. 5*A*).

To explore the mechanisms underlying the pattern of threshold change, we implemented the mathematical model of the human motor axon described in full elsewhere (Bostock *et al.* 1991; Kiernan *et al.* 2005; Kanai *et al.* 2006; Jankelowitz *et al.* 2007*a*). The model motor axon generated threshold behaviour to the complex conditioning stimulus qualitatively similar to that seen in the *in vivo* recordings (Fig. 5*A*, lines). For the same conditioning depolarization, the threshold changes were greater in the model (compare experimental data with the

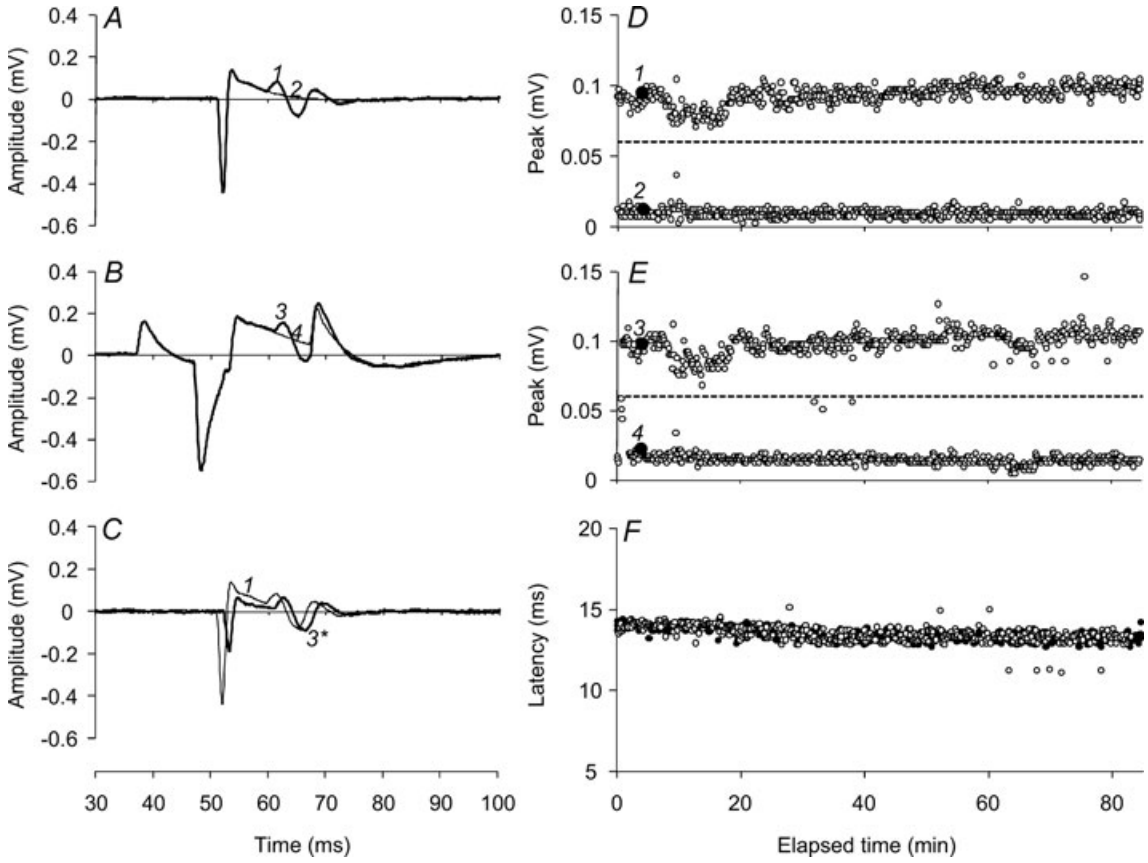

Figure 4. All-or-none response of a single motor axon to the complex conditioning stimulus throughout an entire experiment

A, response of a single motor unit to the 1.0 ms test stimulus (1, thick line). The non-response is labelled 2 (thin line). *B*, response to the test stimulus when it was conditioned (3, thick line). The non-response to the conditioned-test is labelled 4 (thin line). *C*, the response to the conditioned test stimulus, shown in *B*, after the subtraction of the conditioning stimulus artefact, plotted (3*, thick line) on the same axes as the response to the unconditioned test stimulus (shown as 1 in *A*) but offset to facilitate comparison. Note that the stimulus artefact for the conditioned response is less than the control because the threshold for the response at the 1.0 ms conditioning–test interval was reduced (see Fig. 5*A*). *D*, all-or-none measures of the amplitude of the single motor unit showing the responses ('hits') and non-responses ('misses') to the unconditioned test stimulus. The traces plotted in *A* are shown as filled data points labelled 1 and 2, respectively. The trigger level for the response is indicated by the dashed line (0.06 mV). *E*, all-or-none measures of the amplitude of the single motor unit showing the responses and non-responses to the conditioned test stimulus. The traces plotted in *B* are shown as filled data points labelled 3 and 4, respectively. *F*, the latencies of the responses (i.e. the 'hits') to the conditioned test stimulus (○) and the unconditioned test (●) during the entire 85 min experiment.

dashed line in Fig. 5*A*), possibly because filtering by soft tissue attenuated the current reaching axons in the *in vivo* experiments, a view supported by the greater similarity of the model axon's response to a 75% conditioning stimulus (continuous line in Fig. 5*A*).

Figure 5*B* compares the behaviour of the model axon (line) with the data for sensory axons from Fig. 2*A* (filled squares). When scaled to eliminate differences in the magnitude of the changes, the patterns were very similar.

In recordings from single motor units, we then replaced the 3-pulse conditioning stimulus by a simple depolarizing pulse to explore whether the pattern of threshold change was a product of the complex waveform. This was done because the changes in excitability were more complex than reported by Shefner *et al.* (1996) using a 0.2 ms test stimulus, and by Bostock *et al.* (2005), using a 1.0 ms stimulus. With subthreshold rectangular depolarizing stimuli of different duration the changes in threshold for 20 single motor unit recordings were similar to those for sensory axons in Fig. 3 and, apart from the extent of the late hyperpolarizing threshold change, they were also similar to the single motor unit data in Fig. 5*A*. Figure 6*A* shows data for five experiments where full data sets were obtained for the four stimulus durations. There was gradual onset of the threshold decrease, related to the end of the depolarizing pulse. The decrease in threshold was greater the longer the stimulus, and was followed by a late hyperpolarizing threshold change that was greater the longer the pulse (Fig. 6*A*). However, as expected, the late hyperpolarizing change in threshold was less than with the complex stimulus. In these experiments, we also studied the responses to 0.1 ms pulses because previous data indicated that with them the threshold decrease attributable to Na^+ currents could exceed that due to passive electrotonic behaviour of the axons (Bostock *et al.* 2005). The response of single motor units to the subthreshold 1 ms depolarizing stimulus was similar in time course and extent (a 6% threshold decrease) to that reported previously (Bostock *et al.* 2005). The gradual onset of the threshold decrease was not noted in that study, probably because consistent sampling at short conditioning–test intervals was not undertaken.

There were similar findings in the model when the complex conditioning stimulus was replaced by a simple subthreshold depolarizing stimulus of 1 ms duration (Fig. 6*B*). As the width of the depolarizing stimulus increased, there was a growth in the threshold decrease, a shift in its peak and a more rapid decay into a late threshold increase. The threshold changes in the model accurately reproduced those seen with the single motor units (though again they were quantitatively greater).

Underlying currents

A previous study (Bostock *et al.* 2005) had indicated that just-subthreshold stimuli would produce a threshold decrease with two major components: a small 'active' component due to the activation of Na^+ currents, the

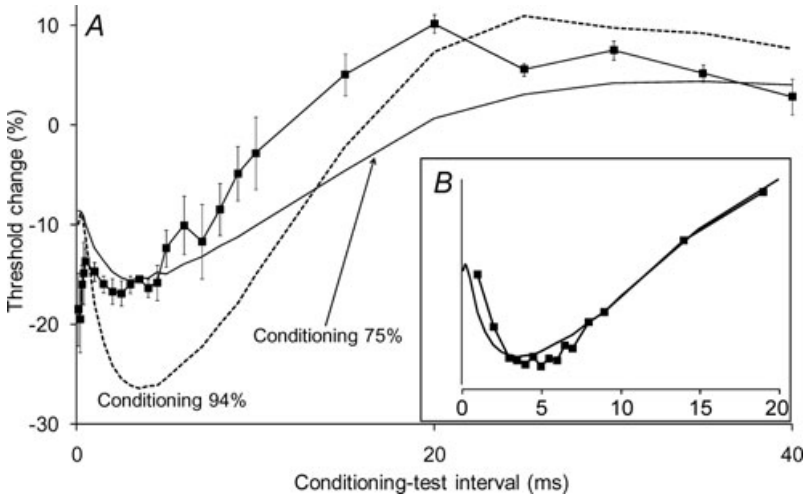

Figure 5. Threshold changes in single motor axons produced by a conditioning stimulus, consisting of a hyperpolarizing pre-pulse, a 5 ms depolarizing pulse and a repolarizing pulse
A, the data points show the threshold changes for three single motor units (from 3 subjects) using 1.0 ms test stimuli. In each instance the depolarizing pulse was 94% of the threshold for the motor unit to a 5 ms stimulus and the repolarizing pulse was 50% of the depolarizing pulse. The 10 ms hyperpolarizing pre-pulse was −30% of the unconditioned 1 ms threshold for the motor unit. Data (■) presented as mean ± S.E.M. ($n = 3$). In this figure and Figs 6 and 7, the end of the depolarizing pulse is aligned to zero on the *x*-axis. Lines show the threshold changes for the model motor axon generated by conditioning stimuli of 75% (continuous line) and 94% (dashed line). The inset panel (*B*) shows the behaviour of sensory axons (data from Fig. 2, ■, 5 ms wide depolarizing pulse) and of the model motor axon, with the data scaled to be of similar magnitude.

extent of which was independent of stimulus duration, and a larger 'passive' component that increased with stimulus duration and was due to the passive electrotonic properties of the axon (Barrett & Barrett, 1982). However, other voltage-dependent conductances should be active in the subthreshold region, and we next considered whether these might have determined the complex pattern of the threshold change seen in the present recordings.

Figure 7 illustrates the changes in membrane potential and the different currents underlying the response of the model axon (dashed line in Fig. 5*A*) to the conditioning stimulus shown above Fig. 7*A*. The underlying changes in membrane potential at the node and internode are shown in Fig. 7*A*; the difference between them drives the current through the Barrett–Barrett resistance (thick dashed line in Fig. 7*B*; see Barrett & Barrett, 1982; Ritchie, 1995). The decrease in threshold following the end of the depolarizing pulse was driven by persistent and transient Na^+ currents which were of similar magnitude in this subthreshold region (Fig. 7*B*). The time course of these Na^+ currents largely followed membrane potential at the node, there being an initial small divergence, attributable to the inactivation gate (Fig. 7*C*). Fast K^+ current was significant, but the slow K^+ current was greater and, with the decay of the Barrett–Barrett current, it largely explained the late hyperpolarizing threshold change. Its onset was unexpectedly early given the slow time course of the activation gate of slow K^+ channels (Fig. 7*C*). However, the changes in the gate were small, starting with the onset of the depolarizing pulse and building up slowly over the subsequent 45 ms. Under these conditions, the time course of slow K^+ current was determined more by the changes in membrane potential at the node.

To determine the contribution of the slow K^+ current to the action potential, the after-potentials and the recovery cycle, the effects of reducing G_{Ks} on the responses of the model were measured. When resting membrane potential of the model axon was not controlled, a reduction in G_{Ks} produced minor changes in the half-width of the action potential, with repetitive firing due to instability occurring when G_{Ks} was less than 2–3% of the standard model. When pump current was adjusted to offset the resting depolarization, reducing G_{Ks} increased the half-width of the action potential by up to 7.2%. These changes in G_{Ks} had much greater effects on the depolarizing after-potential, which was increased by up to 100% (Fig. 8*A*), though (as expected) this was less apparent when membrane potential was allowed to depolarize (trace *d*). The three phases of recovery of excitability following a discharge (i.e. the relative refractory period, the supernormal/superexcitable period and the late subnormal/subexcitable period) were all affected by decreasing G_{Ks} (Fig. 8*B*), but when there was depolarization, as in trace *d*, the increase in superexcitability was reduced.

Discussion

This study demonstrates that a number of processes with differing time courses can explain the threshold behaviour of human myelinated axons when there are subthreshold pertubations to membrane potential, and that the contribution of the different processes varies with the nature and duration of the perturbation. The dominant influence is a decrease in threshold (a form of 'subthreshold superexcitability') that can be attributed to persistent and transient Na^+ currents and the passive electrotonic properties of the axons. The gradual onset of the subthreshold superexcitability largely follows membrane potential, and there is also a decaying contribution from Na^+ channel inactivation. The extent of superexcitability declines due to decay in the leakage current through the Barrett–Barrett resistance and to activation of outward K^+ currents, largely through slow K^+ channels. The active influence was maximized when axons

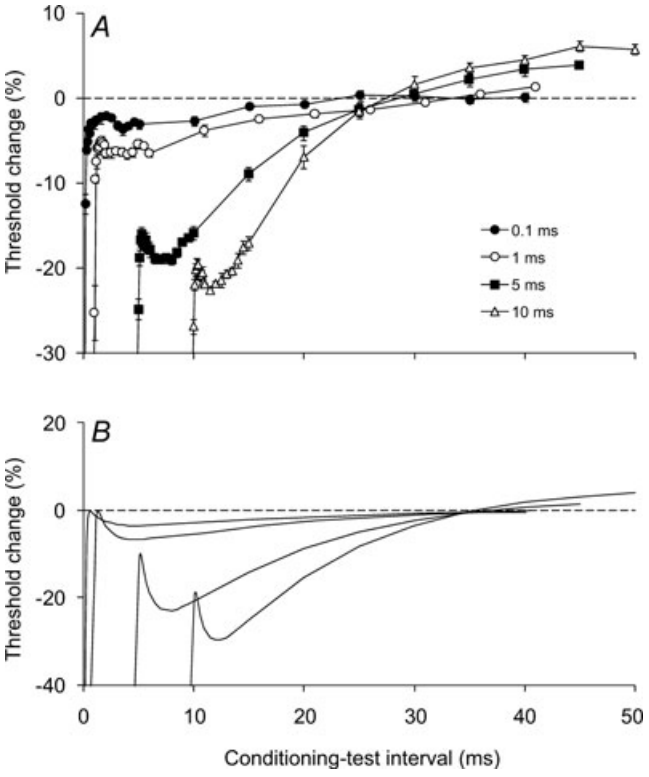

Figure 6. Threshold changes in single motor axons induced by depolarizing pulses of different duration (i.e. conditioning stimuli without both the hyperpolarizing pre-pulses and the partially depolarizing pulses)
A, threshold changes were recorded from single motor units using 1 ms test stimuli. The conditioning depolarizing pulses were 94% of the threshold of the motor unit to a stimulus of the equivalent width. The conditioning depolarization lasted 0.1 ms (●), 1 ms (○), 5 ms (■) or 10 ms (△). Data presented as mean ± S.E.M. of 5 experiments on 3 subjects for each of the four pulse durations. *B*, threshold changes generated by the model axon in response to the depolarizing stimuli used in *A*.

were kept partially depolarized. The modelling indicates that, as expected, a number of currents contribute to the threshold behaviour of human myelinated axons, not just I_{NaP}. These studies provide insight into axonal function under real-life conditions and, in doing so, they raise issues that were not immediately predictable from voltage-clamp data for excised axons. These are addressed below.

Passive properties of axons

Subthreshold superexcitability is dominated by leakage current through the Barrett–Barrett resistance, a conclusion in keeping with that of Shefner *et al.* (1996). In the study of Bostock *et al.* (2005), changes in excitability due to the electrotonic properties outweighed the active channel-dependent changes except with short depolarizing stimuli of less than 0.2 ms duration. In that study, the passive electrotonic properties depended on stimulus charge (and therefore stimulus duration) and dominated the change in excitability produced by subthreshold depolarizing stimuli of 1 ms duration. The active component did not vary with stimulus duration and amounted to only a few per cent. In that study and the present experiments, the passive properties include the fast electrotonic response of nodal origin, proportional to the applied current (Bostock *et al.* 1998), and the response

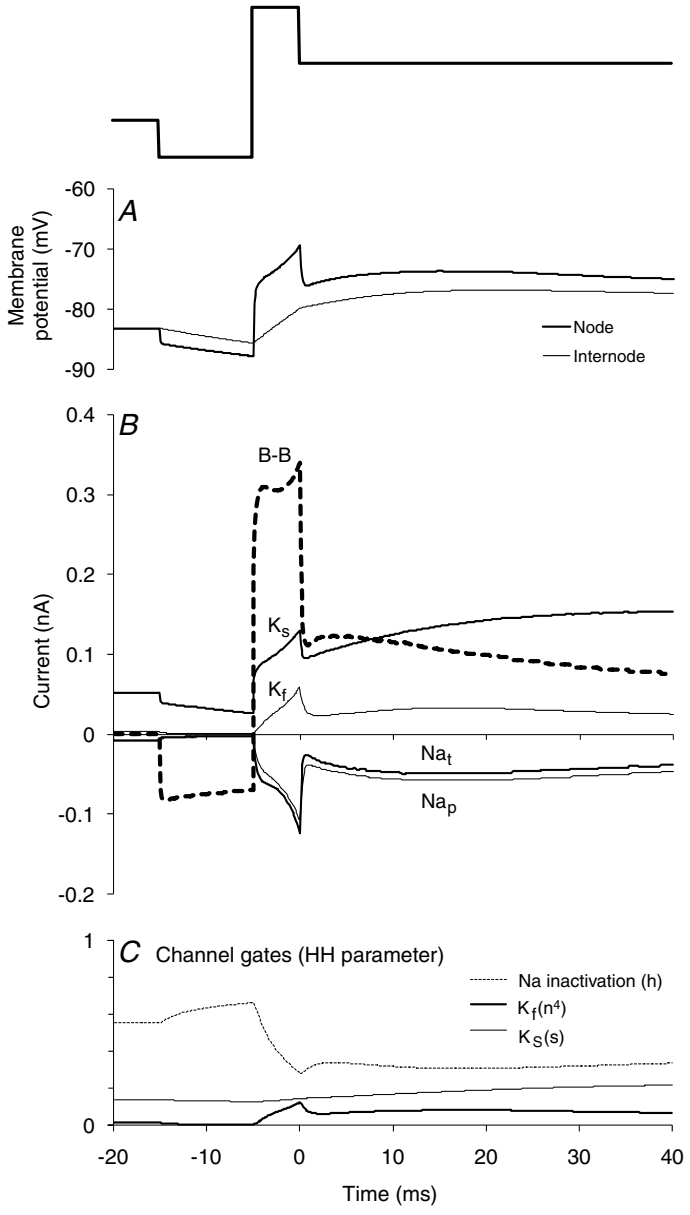

Figure 7. Changes in membrane potential, nodal currents and their gates underlying the threshold changes in Fig. 5*A*

A, changes in membrane potential at the node (thick line) and internode (thin line) generated by the model axon in response to the conditioning stimulus illustrated above the panel. *B*, changes in the key currents (Barrett–Barrett, slow K^+ (K_s), fast K^+ (K_f), transient Na^+ (Na_t) and persistent Na^+ (Na_P)) at the node in response to the conditioning stimulus illustrated above *A*. *C*, corresponding changes in the gating behaviour of key nodal channels as generated by the model axon. The data in *C* emphasize the role of inactivation in limiting the transient Na^+ current at rest and during the different phases of the conditioning stimulus. Note that the slow K^+ gate opens slowly and that channel gating does not limit the contribution of the channel current to the early phases of the conditioning stimulus.

due to the discharge of the internodal capacitance, which steadily charges the longer the applied current (Barrett & Barrett, 1982). The threshold change produced by Na^+ currents is determined by the number of Na^+ channels that fail to inactivate and is smaller than that due to the Barrett–Barrett current. While it was expected that the persistent Na^+ current would account for most of the active component of the threshold decrease, our modelling suggests that transient current makes a similar contribution, though modified by the inactivation gate. With the single units in Fig. 6*A*, the threshold change was 2–3% with 0.1 ms stimuli and ∼22% with 10 ms stimuli. The former represents the upper limit of the contribution of Na^+ currents to the threshold decreases seen in the present recordings.

Currents in intact axons

As indicated in Methods and Results, there are subtle differences in the properties of sensory and motor axons, in part due to greater persistent Na^+ current and greater hyperpolarization-activated current on sensory axons (Bostock & Rothwell, 1997; Bostock *et al.* 1998; Burke *et al.* 2001). It is unlikely that the latter was activated significantly by the stimuli used in this study. However, it is likely that the role of persistent Na^+ current is greater in sensory axons than is indicated by recordings and modelling of data for motor axons. While the present studies allow cogent arguments to be developed, it would be prudent to retain some reservation when extrapolating from indirect data to the underlying currents. Nevertheless, the conclusions of this study do have some support from the pharmacological studies on rat and lizard axons and modelling studies performed by others, as detailed in the following section.

The persistent Na^+ current largely followed the changes in membrane potential, and contributed to the development of subthreshold superexcitability over the first few milliseconds. It was not expected that the change in transient Na^+ current would contribute almost as much as the change in persistent current to the decrease in threshold. Of course, this involves only a small percentage of the total transient Na^+ current, perhaps 1%, similar to the percentage of the total Na^+ current that has been estimated to be persistent in human motor axons (Bostock & Rothwell, 1997). It is also notable that the transient and

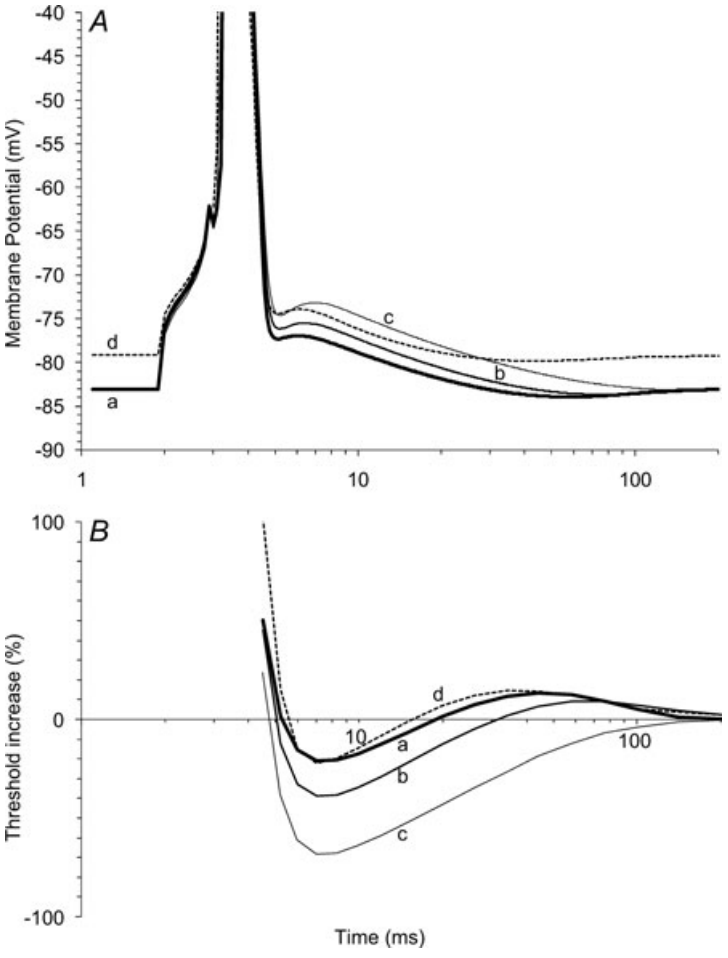

Figure 8. Effects of varying I_{Ks} on the action potential and recovery cycle of the model motor axon
A, the action potential in response to a just-suprathreshold stimulus. Trace *a* (thick line) represents the response of the standard model. In traces *b* and *c*, I_{Ks} was reduced to 50% (*b*) and zero (*c*), but the pre-stimulus membrane potential was clamped to the control level by an offsetting increase in pump current. In trace *d*, pre-stimulus membrane potential was allowed to vary, and I_{Ks} was reduced to 50%. Note the minor changes in duration of the attenuated action potential and the large changes in the depolarizing and hyperpolarizing after-potentials. *B*, the recovery of excitability of the model axon following the action potentials shown in *A*. Note the profound effect on superexcitability and (as expected) late subexcitability when the prestimulus membrane potential was clamped, and the minor changes when it was not clamped. The 4 mV depolarizing shift in membrane potential is associated with an increase in the relative refractory period and lesser superexcitability (though this is still enhanced for membrane potential).

persistent Na^+ currents were of comparable magnitude at rest. The importance of inactivation of the transient current, even at subthreshold membrane potentials, is emphasized by the model results in Fig. 7*C*. Recovery from inactivation contributes to the development of subthreshold superexcitability following the depolarizing pulse, and residual inactivation limits the contribution of transient Na^+ currents during the maintained partial depolarization.

The Barrett–Barrett resistance has been modelled as an ohmic pathway between the node and internode, passing a current proportional to the difference between the nodal and internodal membrane potentials. This current can be quite large, even with subthreshold perturbations to membrane potential, as shown in Fig. 7*B*, and it will be an important factor in any induced changes in membrane potential.

In experiments on human nerve *in vivo*, axons are, of necessity, not under voltage-clamp conditions. The current through a voltage-dependent channel is then dependent on membrane potential in addition to the gating properties of the channel. The change in gating of slow K^+ channels is truly slow (Fig. 7*C*), such that the changes in current through the channel were determined mainly by membrane potential, at least over the early intervals. This explains the magnitude of the slow K^+ current early after the onset of the depolarizing pulse at a time when the channel gate was slowly opening.

K^+ currents and the recovery of axonal excitability following a discharge

We have referred to two K^+ currents, fast and slow, following Baker *et al.* (1987) and Röper & Schwarz (1989), and in accordance with previous studies, including *in vivo* studies on human nerve (Bostock *et al.* 1998; Burke *et al.* 2001). This usage does not imply specific channel subtypes. There are generally considered to be three K^+ currents in mammalian myelinated axons (Jonas *et al.* 1989): I_{Ks} (slow), I_{Kf1} (intermediate) and I_{Kf2} (fast). At least five K^+ channel subtypes with overlapping properties contribute to these macroscopic currents in human myelinated axons (Reid *et al.* 1999). I_{Kf1} has a voltage dependence that overlaps that of I_{Ks} but has intermediate/fast kinetics, while I_{Kf2} activates at more positive potentials and has faster kinetics. It is unlikely that subthreshold stimuli would activate the latter significantly, and most of the current termed 'fast' in this paper was probably I_{Kf1}. Pharmacological blockade of fast K^+ currents with 4-aminopyridine produces a depolarizing shift in membrane potential comparable to that produced by blocking slow K^+ currents (Grafe *et al.* 1994), supporting the view that K^+ channels with intermediate or fast kinetics contribute to the threshold behaviour of myelinated axons.

Using voltage- (and current-) clamped data, repolarization after an action potential in rat and human myelinated axons can be modelled accurately using only two parameters: inactivation of Na^+ channels and current leakage (e.g. Chiu *et al.* 1979; Schwarz *et al.* 1995). It is therefore generally assumed that recovery after the absolute refractory period does not involve voltage-dependent K^+ currents (see Ritchie, 1995; Bostock *et al.* 1998; Burke *et al.* 2001). This is consistent with the concentration of K^+ channels with fast kinetics in the juxta-paranodal region (Brismar, 1980; Chiu & Ritchie, 1981; Röper & Schwarz, 1989), and the slow gating of slow K^+ channels (Röper & Schwarz, 1989). Paranodal fast K^+ channels are activated following a single action potential (David *et al.* 1993), and they will affect the depolarizing after-potential, but whether they influence repolarization at the node is conjectural.

A channel gate may act as a brake on the channel current but, in the present experiments, the slow gating of slow K^+ channels did not prevent the relatively small changes in membrane potential from driving a significant current early after the end of the depolarizating pulse. Approximately 35% of slow K^+ channels are open at resting membrane potential (Röper & Schwarz, 1989), and it is likely that the extreme perturbation to membrane potential associated with axonal discharge would drive a slow K^+ current that largely parallels membrane potential as the gate slowly opens. The conclusion that slow K^+ currents may be active early during and after an action potential is not consistent with conclusions from experiments using tetraethyl ammonium (TEA). TEA is said to have little effect on the duration of the action potential of axons in the optic nerve or nerve root of rats (Bostock *et al.* 1981; Kocsis *et al.* 1987; Eng *et al.* 1988; Gordon *et al.* 1988), but TEA may have produced a depolarizing shift in membrane potential, and this would have altered both Na^+ channel inactivation and the depolarizing after potential (Fig. 8). In lizard axons, the addition of TEA after aminopyridines produces a further increase in the width of the action potential (David *et al.* 1995), indicating that slow kinetics do not prevent an effective early current. The only quantitative data on the effects of TEA on action potential half-width are from Bostock *et al.* (1981), and they indicate an increase of compound potential duration by, on average, 8.6% with 20 mM TEA and 11.2% with 60 mM TEA (with smaller changes for single units using 10 mM TEA). It is possible that I_{Ks} contributes to repolarization under natural conditions but, even if it does not, the slow gating of these channels does not prevent an early action, affecting the after-potentials and related phases of the recovery cycle, particularly the depolarizing after-potential and the

extent of superexcitability (Fig. 8*B*; see also McIntyre *et al.* 2002).

Clinical implications

The abnormalities of nerve excitability that are associated with the development of neuropathy are now being investigated in clinical settings, using threshold tracking techniques (Bostock *et al.* 1998; Burke *et al.* 2001; Krishnan *et al.* 2008). The excitability changes recorded from patients are often complex, and it is only through mathematical modelling that a better understanding of the pathophysiology of neuropathy may be developed. To date, the mathematical simulations have involved a model of the human axon derived from voltage clamp data (Bostock *et al.* 1991, 1995; Schwarz *et al.* 1995; Kiernan *et al.* 2005; Jankelowitz *et al.* 2007*a*). Awareness that human nodal slow K^+ currents may be activated and could contribute to the early changes in excitability following an impulse, may potentially facilitate a clearer understanding and thereby interpretation of the excitability changes recorded from neuropathic patients.

References

Bae JS, Sawai S, Misawa S, Kanai K, Isose S, Shibuya K & Kuwabara S (2008). Effects of age on excitability properties in human motor axons. *Clin Neurophysiol* **119**, 2282–2286.

Baker M, Bostock H, Grafe P & Martius P (1987). Function and distribution of three types of rectifying channel in rat spinal root myelinated axons. *J Physiol* **383**, 45–67.

Barrett EF & Barrett J (1982). Intracellular recording from vertebrate myelinated axons: mechanism of the depolarizing afterpotential. *J Physiol* **323**, 117–144.

Blight AR (1985). Computer simulation of action potentials and after potentials in mammalian myelinated axons: the case for a lower resistance myelin sheath. *Neuroscience* **15**, 13–31.

Blight AR & Someya S (1985). Depolarizing after potentials in myelinated axons of mammalian spinal cord. *Neuroscience* **15**, 1–12.

Bostock H (1983). The strength–duration relationship for excitation of myelinated nerve: Computed dependence on membrane parameters. *J Physiol* **341**, 59–74.

Bostock H & Baker M (1988). Evidence for two types of potassium channel in human motor axons *in vivo*. *Brain Res* **462**, 354–358.

Bostock H, Baker M & Reid G (1991). Changes in excitability of human motor axons underlying post-ischaemic fasciculations: evidence for two stable states. *J Physiol* **441**, 537–557.

Bostock H, Cikurel K & Burke D (1998). Threshold tracking techniques in the study of human peripheral nerve. *Muscle Nerve* **21**, 137–158.

Bostock H, Lin CS-Y, Howells J, Trevillion L, Jankelowitz S & Burke D (2005). After-effects of near-threshold stimulation in single human motor axons. *J Physiol* **564**, 931–940.

Bostock H & Rothwell JC (1997). Latent addition in motor and sensory fibres of human peripheral nerve. *J Physiol* **498**, 277–294.

Bostock H, Sears TA & Sherratt RM (1981). The effects of 4-aminopyridine and tetraethylammonium ions on normal and demyelinated mammalian nerve fibres. *J Physiol* **313**, 301–315.

Bostock H, Sharief MK, Reid G & Murray NM (1995). Axonal ion channel dysfunction in amyotrophic lateral sclerosis. *Brain* **118**, 217–225.

Bowe CM, Kocsis JD & Waxman SG (1987). The association of the supernormal period and the depolarizing afterpotential in myelinated frog and rat sciatic nerve. *Neuroscience* **21**, 585–593.

Brismar T (1980). Potential clamp analysis of membrane currents in rat myelinated nerve fibres. *J Physiol* **298**, 171–184.

Burke D, Kiernan MC & Bostock H (2001). Excitability of human axons. *Clin Neurophysiol* **112**, 1575–1585.

Chiu SY & Ritchie JM (1981). Evidence for the presence of potassium channels in the paranodal region of acutely demyelinated mammalian single nerve fibres. *J Physiol* **313**, 415–431.

Chiu SY, Ritchie JM, Rogart RB & Stagg D (1979). A quantitative description of membrane currents in rabbit myelinated nerve. *J Physiol* **292**, 149–166.

David G, Barrett JN & Barrett EF (1993). Activation of intermodal potassium conductance in rat myelinated axons. *J Physiol* **472**, 177–202.

David G, Modney B, Scappaticci KA, Barrett JN & Barrett EF (1995). Electrical and morphological factors influencing the depolarizing after-potential in rat and lizard myelinated axons. *J Physiol* **489**, 141–157.

Eng DL, Gordon TR, Kocsis JD & Waxman SG (1988). Development of 4-AP and TEA sensitivities in mammalian myelinated nerve fibers. *J Neurophysiol* **60**, 2168–2179.

Gordon TR, Kocsis JD & Waxman SG (1988). Evidence for the presence of two types of potassium channels in the rat optic nerve. *Brain Res* **447**, 1–9.

Grafe P, Bostock H & Schneider U (1994). The effects of hyperglycaemic hypoxia on rectification in rat dorsal root axons. *J Physiol* **480**, 297–307.

Hales JP, Lin CS-Y & Bostock H (2004). Variations in excitability of single human motor axons, related to stochastic properties of nodal sodium channels. *J Physiol* **559**, 953–964.

Iglesias C, Marchand-Pauvert V, Lourenço G, Burke D & Pierrot-Deseilligny E (2007). Task-related changes in propriospinal excitation from hand muscles to human flexor carpi radialis motoneurones. *J Physiol* **582**, 1361–1379.

Jankelowitz SK, Howells J & Burke D (2007*a*). Plasticity of inwardly rectifying conductances following a corticospinal lesion in human subjects. *J Physiol* **581**, 927–940.

Jankelowitz SK, McNulty PA & Burke D (2007*b*). Changes in measures of motor axon excitability with age. *Clin Neurophysiol* **118**, 1397–1404.

Jonas P, Bräu ME, Hermsteiner M & Vogel W (1989). Single-channel recording in myelinated nerve fibers reveals one type of Na channel but different K channels. *Proc Nat Acad Sci U S A* **86**, 7238–7242.

Kanai K, Kuwabara S, Misawa S, Tamura N, Ogawara K, Nakata M, Sawai S, Hattori T & Bostock H (2006). Altered axonal excitability properties in amyotrophic lateral sclerosis: impaired potassium channel function related to disease stage. *Brain* **129**, 953–962.

Kiernan MC, Burke D, Andersen KV & Bostock H (2000). Multiple measures of axonal excitability: a new approach in clinical testing. *Muscle Nerve* **23**, 399–409.

Kiernan MC, Isbister GK, Lin CS-Y, Burke D & Bostock H (2005). Acute tetrodotoxin-induced neurotoxicity after ingestion of puffer fish. *Ann Neurol* **57**, 339–348.

Kiernan MC, Lin CS-Y, Andersen KV, Murray NM & Bostock H (2001). Clinical evaluation of excitability measures in sensory nerve. *Muscle Nerve* **24**, 883–892.

Kocsis JD, Eng DL, Gordon TR & Waxman SG (1987). Functional differences between 4-aminopyridine and tetraethylammonium-sensitive potassium channels in myelinated axons. *Neurosci Lett* **75**, 193–198.

Krishnan AV, Lin CS-Y, Park SB & Kiernan MC (2008). Assessment of nerve excitability in toxic and metabolic neuropathies. *J Peripher Nerv Syst* **13**, 7–26.

Lin CS-Y, Kiernan MC, Burke D & Bostock H (2006). Assessment of nerve excitability properties in peripheral nerve disease. In *Handbook of Clinical Neurophysiology*, Vol. 7, *Clinical Neurophysiology of Peripheral Nerve Diseases*, ed. Kimura J, series ed. Daube JR & Mauguière F, pp. 381–403. Elsevier, Amsterdam.

McIntyre CC, Richardson AG & Grill WM (2002). Modeling the excitability of mammalian nerve fibers: influence of afterpotentials on the recovery cycle. *J Neurophysiol* **87**, 995–1006.

Magistretti J, Castelli L, Forti L & D'Angelo E (2006). Kinetic and functional analysis of transient, persistent and resurgent sodium currents in rat cerebellar granule cells *in situ*: an electrophysiological and modelling study. *J Physiol* **573**, 83–106.

Mogyoros I, Kiernan M & Burke D (1996). Strength-duration properties of human peripheral nerve. *Brain* **119**, 439–447.

Raman IM & Bean BP (1997). Resurgent sodium current and action potential formation in dissociated cerebellar purkinje neurons. *J Neurosci* **17**, 4517–4526.

Raman IM & Bean B (2001). Inactivation and recovery of sodium currents in cerebellar purkinje neurons: evidence for two mechanisms. *Biophys J* **80**, 729–737.

Reid G, Scholz A, Bostock H & Vogel W (1999). Human axons contain at least five types of voltage-dependent potassium channel. *J Physiol* **518**, 681–696.

Ritchie JM (1995). Physiology of axons. In *The Axon: Structure, Function and Pathophysiology*, ed. Waxman SG, Kocsis JD & Stys PK, pp. 68–96. Oxford University Press, New York.

Röper J & Schwarz JR (1989). Heterogeneous distribution of fast and slow potassium channels in myelinated rat nerve fibres. *J Physiol* **416**, 93–110.

Schwarz JR, Reid G & Bostock H (1995). Action potentials and membrane currents in the human node of Ranvier. *Pflugers Arch* **430**, 283–292.

Shefner JM, Preston DC & Logigian EL (1996). Activity-dependent conduction in single motor units. *Neurology* **46**, 1387–1390.

Weiss G (1901). Sur la possibilité de rendre comparables entre eux les appareils servant à l'excitation életrique. *Arch Ital Biol* **35**, 413–446.

Acknowledgements

The authors are grateful to Professor Hugh Bostock for advice and for suggestions on an early draft of this manuscript. This study was supported by the National Health and Medical Research Council and the Australian Research Council.